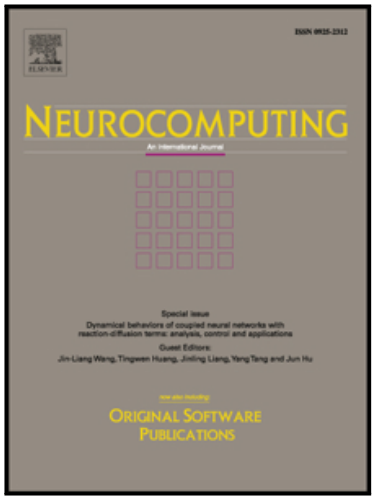
CORA Cork Open Research Archive
Cartlann Taighde Oscailte Chorcaí

Title	Vibrational resonance in a scale-free network with different coupling schemes
Authors	Agaoglu, Sukriye Nihal;Calim, Ali;Hövel, Philipp;Ozer, Mahmut;Uzuntarla, Muhammet
Publication date	2018-10-05
Original Citation	Agaoglu, S. N., Calim, A., Hövel, P., Ozer, M. and Uzuntarla, M. (2019) 'Vibrational resonance in a scale-free network with different coupling schemes', Neurocomputing, 325, pp. 59-66. doi: 10.1016/j.neucom.2018.09.070
Type of publication	Article (peer-reviewed)
Link to publisher's version	http://www.sciencedirect.com/science/article/pii/S0925231218311512 - 10.1016/j.neucom.2018.09.070
Rights	© 2018 Elsevier B.V. All rights reserved. This manuscript version is made available under the CC BY-NC-ND 4.0 licence. - https://creativecommons.org/licenses/by-nc-nd/4.0/
Download date	2024-03-28 20:15:22
Item downloaded from	https://hdl.handle.net/10468/9646

UCC
University College Cork, Ireland
Coláiste na hOllscoile Corcaigh

Communicated by Dr. J. Torres

Accepted Manuscript



Vibrational Resonance in a Scale-Free Network with Different Coupling Schemes

Sukriye Nihal Agaoglu, Ali Calim, Philipp Hövel, Mahmut Ozer, Muhammet Uzuntarla

PII: S0925-2312(18)31151-2
DOI: https://doi.org/10.1016/j.neucom.2018.09.070
Reference: NEUCOM 20003

To appear in: *Neurocomputing*

Received date: 17 July 2018
Revised date: 17 September 2018
Accepted date: 26 September 2018

Please cite this article as: Sukriye Nihal Agaoglu, Ali Calim, Philipp Hövel, Mahmut Ozer, Muhammet Uzuntarla, Vibrational Resonance in a Scale-Free Network with Different Coupling Schemes, *Neurocomputing* (2018), doi: https://doi.org/10.1016/j.neucom.2018.09.070

This is a PDF file of an unedited manuscript that has been accepted for publication. As a service to our customers we are providing this early version of the manuscript. The manuscript will undergo copyediting, typesetting, and review of the resulting proof before it is published in its final form. Please note that during the production process errors may be discovered which could affect the content, and all legal disclaimers that apply to the journal pertain.

ACCEPTED MANUSCRIPT

Vibrational Resonance in a Scale-Free Network with Different Coupling Schemes

Sukriye Nihal Agaoglu,[1] Ali Calim,[2] Philipp Hövel,[3]
Mahmut Ozer,[1] and Muhammet Uzuntarla[2,*]

[1]*Department of Electrical and Electronics Engineering, Bulent Ecevit University, Engineering Faculty, 67100 Zonguldak, Turkey*

[2]*Department of Biomedical Engineering, Bulent Ecevit University, Engineering Faculty, 67100 Zonguldak, Turkey*

[3]*School of Mathematical Sciences, Western Gateway Building, Western Road University College Cork, Cork, T12 XF62, Ireland*

Abstract

We investigate the phenomenon of vibrational resonance (VR) in neural populations, whereby weak low-frequency signals below the excitability threshold can be detected with the help of additional high-frequency driving. The considered dynamical elements consist of excitable FitzHugh-Nagumo neurons connected by electrical gap junctions and chemical synapses. The VR performance of these populations is studied in unweighted and weighted scale-free networks. We find that although the characteristic network features – coupling strength and average degree – do not dramatically affect the signal detection quality in unweighted electrically coupled neural populations, they have a strong influence on the required energy level of the high-frequency driving force. On the other hand, we observe that unweighted chemically coupled populations exhibit the opposite behavior, and the VR performance is significantly affected by these network features whereas the required energy remains on a comparable level. Furthermore, we show that the observed VR performance for unweighted networks can be either enhanced or worsened by degree-dependent coupling weights depending on the amount of heterogeneity.

Keywords: Vibrational Resonance; weighted networks; chemical synapses; gap junctions

*Electronic address: muzuntarla@yahoo.com(M.Uzuntarla)

ACCEPTED MANUSCRIPT

I. INTRODUCTION

The ability of weak-signal detection and transmission of nonlinear systems is crucial to understand the processing of information in many complex structures in nature. Over the last few decades, much attention has been devoted to stochastic resonance (SR), which manifests itself as detection and transmission of weak-signals in the presence of noise [1, 2]. In a large variety of artificial and natural nonlinear dynamical systems, including physical and biological ones, it is observed that the presence of an optimal level of noise leads to maximal correlation between the input signal and the system's response [3–12]. However, due to the random nature of noise, researchers have been looking for alternatives to obtain similar signal detection performances. Recently, it has been shown that the response of a nonlinear system to a weak low-frequency signal can be enhanced by an additional high-frequency input, which then has a role similar to noise in SR. This SR-like phenomenon is known as vibrational resonance (VR). Then, the response of a nonlinear system results in a bell-shaped dependence on amplitude of the high-frequency driving signal, indicating that the correlation between the signal and the system's response is maximal around a moderate vibration force [13]. It is worth to note that VR is a different concept than classical vibrational control theory [14–16]. Although, VR and vibrational control have in common that the system's performance is enhanced due to an additional high-frequency driving, the purpose, however, is of different nature: The aim of vibrational control is the stabilization of unstable (steady) states, while vibrational resonance will drive the system away from its fixed point.

In recent years, there has been a growing interest in studying VR in excitable neuronal systems [17, 18]. The reasons are manifold: The presence of such bichromatic signals with widely separated frequencies is very common in the internal and surrounding environment of living organisms [19–24]. Furthermore, neurons are generally subject to multiple signals of, for instance, sensory or motor information that can range from milliseconds to days. Another remarkable example is the dynamical behavior of bursting neurons, which operates on two different time scales [25]. Moreover, the effect of high-frequency stimulation in treatments of neurological disorders, i.e., Parkinson and epilepsy, can be studied in the framework of VR in neuronal systems [26, 27].

Motivated by the above mentioned reasons, various works have investigated VR in neu-

ronal systems at the level of both a single neuron and networks under different biophysical conditions. For instance, Ullner et al. studied VR in a single FitzHugh-Nagumo model and showed that the optimal amplitude of the high-frequency signal can indeed increase the response of the neuron to a low-frequency signal [28]. They also showed that high-frequency driving can substitute a fraction of the noise and hence control the SR performance via the VR mechanism. Wu et al. [26] studied VR in a more realistic model neuron, i.e., the Hodgkin-Huxley system. Comparing to VR in models with constant ion concentrations, they observed significantly enhanced vibrational multi-resonances for a single neuron where the potassium and sodium ion concentrations vary temporally. On the level of neural populations, VR has been investigated extensively for different coupling topologies including feed-forward [29–31], random [18, 32] and small-world networks [33, 34]. The vast majority of these studies reported the emergence of VR under the variation of population features such as the population size, complexity of topology, synaptic coupling type, and local neuronal dynamics. Apart from these works, as a first attempt, we have recently studied VR in a scale-free (SF) network, which is a well-known and widely-used connectivity paradigm in computational studies of local microcircuits since such connectivity has been observed in many functional brain regions via neuroimaging and electrophysiological studies [35–38]. We demonstrated that VR can also emerge in a SF neuronal network for a wide range of system parameters. Moreover, it was shown that neuronal heterogeneity in this type of networks may give rise to a different VR behavior compared to homogeneous populations in terms of the signal encoding quality and required energy level [39].

Here, we continue to study the VR phenomenon in SF networks by considering electrically and chemically coupled neural populations. In fact, it should be noted that VR dynamics in neural populations consisting of electrical and chemical couplings have been studied in several previous works [29, 32, 34], in which various types of VR behavior have been reported for different network types. This plurality of reported results indicates that the influence of electrical and chemical synaptic couplings on VR is highly associated with network features (i.e. topology, network size, average degree and complexity). For instance, a coupling scheme may enhance VR performance of a population with a given network topology whereas the same coupling may worsen it with another type of topology. This relation also holds for SR phenomenon in neuronal systems, as many reported findings indicate that the noise-assisted weak signal detection ability of electrically and chemically coupled populations is peculiar to

ACCEPTED MANUSCRIPT

different network states [40–44]. Therefore, it is difficult to conclude that one coupling type is vastly superior to another when considering SR and VR phenomena in neuronal networks. Since the precise roles of different types of coupling in shaping VR performance in SF networks are still not completely established, our aim is to investigate the conditions for the emergence of VR in SF networks of neurons coupled via electrical and chemical synapses. This will fill a gap with respect to the importance of this relevant network topology. On the other hand, recent publications on the VR phenomenon in neural populations have entirely focused on unweighted networks, where each link between coupled neurons is realized with a fixed coupling strength. However, this is a simplification of the peculiarities of an actual neural medium since findings from imaging studies have demonstrated that neural populations have not only complex connection topologies but also weighted communication paths. This also holds for many real-world networks, e.g. transportation, social and other biological systems such as gene and protein interaction networks [45–49]. Therefore, investigating the VR dynamics of electrically and chemically coupled population in a weighted SF network is of great importance.

In what follows, firstly, the emergence of VR in unweighted electrically and chemically coupled populations is demonstrated comparatively as a function of key system parameters, i.e., coupling strength and link density. Then, we systematically investigate the effect of weighted coupling on the VR performance in both cases and conclude in Sec. IV with a summary.

II. MODELS AND METHODS

We consider a population of identical $N = 200$ neurons. The dynamics of each neuron in the population are modeled by the well established FitzHugh-Nagumo equations [50]. This is a convenient neural system for investigating the VR phenomenon due to its simplicity to control the excitability and its computational efficiency. This simple but paradigmatic model mimics the main firing characteristics of neuronal activities of excitability type II. The equations of the FitzHugh-Nagumo model in a population are given by:

$$\epsilon \frac{dx_i(t)}{dt} = x_i(t) - \frac{x_i(t)^3}{3} - y_i(t) + I_i^{\mathrm{syn}}(t) \tag{1a}$$

$$\frac{dy_i(t)}{dt} = x_i(t) + a + I_i^{\mathrm{stim}}(t). \tag{1b}$$

The dimensionless variables x_i and y_i denote a fast activation variable that represents the voltage of the membrane, and a slow recovery variable that inhibits the activator, respectively. The parameter ϵ is very small and separates their time scales. The value of the time scale ratio is set to $\epsilon = 0.01$. The excitability level of each neuron is determined by the bifurcation (control) parameter a. The uncoupled FitzHugh-Nagumo neuron is excitable for $|a| > 1$ and the system has a stable fixed point $(x_i^*, y_i^*) = (-a, -a + a^3/3)$. This fixed point becomes unstable for $|a| < 1$. Then, the system exhibits an oscillatory behavior generating regular spikes. In the following, the bifurcation parameter is set to $a = 1.05$ for all neurons in the network, because we are interested in the weak-signal detection performance of the neurons in their excitable regime.

The external stimulus current I_i^{stim} applied to neuron i is a bichromatic signal consisting of a subthreshold low-frequency signal (LFS) and a high-frequency stimulus (HFS) modeled as $I_i^{\text{stim}}(t) = A\cos(\omega t) + B\cos(\Omega t + \phi_i)$ where A and ω (B and Ω) refer to the LFS (HFS) amplitude and angular frequency, respectively. We choose a LFS amplitude of $A = 0.01$ so that the system remains below the excitation threshold in the presence of LFS alone, and $\Omega \gg \omega$, in particular $\Omega = 5$ and $\omega = 0.1$. The initial HFS phases ϕ_i are randomly drawn from a uniform distribution between $[0\ \pi]$.

In Eq. (1a), the coupling term I_i^{syn} is the total synaptic current received by neuron i. It includes electrical or chemical synapses. In the case of electrical gap junctions, the coupling is proportional to the sum of the difference between membrane voltage of neuron i and that all of its neighbors $j \in N(i)$ and can be described by:

$$I_i^{\text{syn}}(t) = \sum_{j \in N(i)} g_e \left(x_j(t) - x_i(t)\right), \tag{2}$$

where g_e is the electrical synaptic strength between neurons i and j. Chemical synapses have more complex and nonlinear dynamics that arise from mechanisms underlying the modulation of the presynaptic neurotransmitter release and postsynaptic binding to a neuroreceptor. Then, the total synaptic current takes the following form:

$$I_i^{\text{syn}}(t) = \sum_{j \in N(i)} g_c\, s_j(t) \left(E_{\text{rev}} - x_i(t)\right), \tag{3}$$

where s_j is determined by

$$\frac{ds_j(t)}{dt} = -\frac{s_j(t)}{\tau_{\text{syn}}} + \sum_{l=1}^{n_j} \delta\left(t - t_l^{(j)}\right). \tag{4}$$

ACCEPTED MANUSCRIPT

Here, g_c is the maximal chemical synaptic strength. s_j is the fraction of open channels of the neuron j. Once the presynaptic neuron j triggers an action potential at times $t_1^{(j)}, \ldots, t_{n_j}^{(j)}$, all synaptic channels open and the fraction s_j is set to $s_j = 1$ via the δ-function. Then, it decays exponentially with a fixed time constant $\tau_{\text{syn}} = 0.83$. E_{rev} is the excitatory synaptic reversal potential and it is assumed to be zero.

As connection topology of the neural population, we consider potentially weighted SF networks. This is a well-known and widely-used connectivity model in computational studies of neuroscience, since many neuroimaging and electrophysiological studies in recent years have revealed that many functional brain regions often exhibit such a topology [35–38, 51]. Graph-based analyses of resting-state fMRI data have also suggested an efficient organization of intrinsic brain connectivity networks, indicating that the human brain is not just represented by binary networks, but also weighted interactions [52–54]. The most prominent construction protocol for a SF network is based on preferential attachment and known as the Barabási-Albert model [55]. This procedure starts with a set of m fully connected nodes, and at each step a new node is introduced that connects to m different nodes already present in the network with a degree-dependent probability Π, such that $\Pi = k_i / \sum_j k_j$ where k_i and k_j are the degrees of nodes i and j, respectively. This procedure yields a network with an average degree k_{avg}, and a power-law degree distribution $P(k) \sim k^{-3}$. In our setup, unless otherwise stated, our SF networks consist of $N = 200$ nodes with one neuron at each node. In addition, to incorporate the coupling weights in the network interactions, we assign weights to links based on the node degrees. We assume the weight associated the link between two nodes to be $w_{ij} = (k_i k_j)^{-\alpha}$ [56]. Then, the value of synaptic strength between two connected neurons becomes $g_e = w_{ij} g_e$ for electrical coupling and $g_c = w_{ij} g_c$ for chemical coupling. Finally, α is a tunable parameter characterizing the weight distribution and the amount of heterogeneity. Unweighted networks are recovered for $\alpha = 0$.

To evaluate the effect of VR on the network, the collective temporal behavior is measured by calculating the average membrane voltage

$$x_{\text{avg}}(t) = \frac{1}{N} \sum_{i=1}^{N} x_i(t), \tag{5}$$

where $x_i(t)$ is the time series of each FHN neuron simulated for $n = 100$ periods of the low-frequency signal ($T = 2\pi/\omega$). The response of the network output to the low-frequency

signal is quantified by means of the Q factor [13]:

$$Q = \sqrt{Q_{\sin}^2 + Q_{\cos}^2}, \tag{6}$$

where $Q_{\sin}$ and $Q_{\cos}$ are computed via the Fourier coefficients after eliminating a sufficiently large transients, T_0:

$$Q_{\sin} = \frac{1}{nT} \int_{T_0}^{T_0+nT} 2\, x_{\text{avg}}(t) \sin(\omega t) dt \tag{7a}$$

$$Q_{\cos} = \frac{1}{nT} \int_{T_0}^{T_0+nT} 2\, x_{\text{avg}}(t) \cos(\omega t) dt. \tag{7b}$$

Q is a measure of the Fourier spectrum of x_{avg} at the frequency ω. With this value, we can test the response of the network to the low-frequency signal. The described mathematical model is integrated numerically using the forward Euler method with a time step $\Delta t = 0.001$. The simulations presented below have been averaged over 20 realizations of the network for any given set of the model parameters.

III. RESULTS

In this section, we will systematically analyze the emergence of VR in electrically and chemically coupled populations of FitzHugh-Nagumo neurons. The VR dynamics of these two types of populations will be investigated in both unweighted and weighted network configurations. For comparison, we first study VR in unweighted networks.

Since the density of links is a crucial property in determining the dynamics and complexity of a network, the weak-signal detection ability of electrically and chemically coupled populations will be analyzed in networks of different link densities. For this purpose, we compute the input-output correlation measure Q for various connectivity levels and fixed coupling strengths as a function of the high-frequency driving amplitude B and, by varying the average degree k_{avg} as the control parameter.

Figure 1 shows the obtained results in both electrically and chemically coupled populations. In electrically coupled unweighted population, the density of connections in the network has no prominent effect on the weak LFS encoding performance since the resulting maximal values $Q_{\max}$ remain constant independent of k_{avg} (Fig. 1a). Additionally, it can be observed that the increase in k_{avg} induces an increase of the optimal driving amplitude B_{opt} corresponding to the peak $Q_{\max}$. This indicates that it requires more energy to obtain the

ACCEPTED MANUSCRIPT

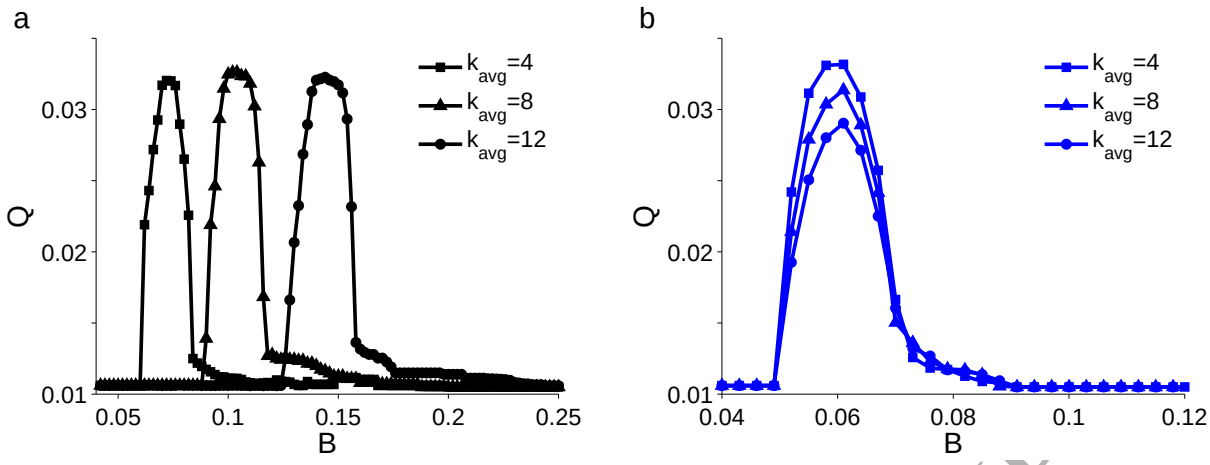


Figure 1: Emergence of vibrational resonance in unweighted electrically and chemically coupled neural populations. The panels show the variation of the amplification factor Q as a function of high-frequency driving amplitude B for different average degrees in (a) electrically coupled and (b) chemically coupled unweighted networks. Model parameters: $g_e = g_c = 0.03$, $\alpha = 0$, $A = 0.01$, $\Omega = 5$, and $\omega = 0.1$.

same signal detection performance in the presence of dense connectivity in an electrically coupled network. On the other hand, a different effect appears in the case of chemically coupled unweighted populations. Figure 1b shows that although the required energy level does not change very much, the signal detection performance slightly decreases as k_{avg} increases. These findings indicate that for fixed coupling strengths, the density of connections in a SF network influences the VR dynamics distinctly in these two types of populations. In particular, the link density plays a key role for the required energy consumption in an electrically coupled population, whereas it is important in a chemically coupled population for determining the efficiency of weak-signal detection.

To generalize above findings, it is important to elaborate further on the results for different synaptic coupling strengths of electrically and chemically coupled populations. To do so, we calculate the optimal required energy level B_{opt} and the maximal amplification factor Q_{max} as a function of g_{e} and g_{c} separately for different k_{avg} values. Figure 2 features the obtained results. It can be seen that the variation of synaptic coupling strengths g_{e} and g_{c} dramatically enhance the effects of k_{avg} for both types of coupling. More precisely, as g_{e} increases, the optimal high-frequency driving force amplitude required for similar VR performance increases in the electrically coupled population. This effect becomes more

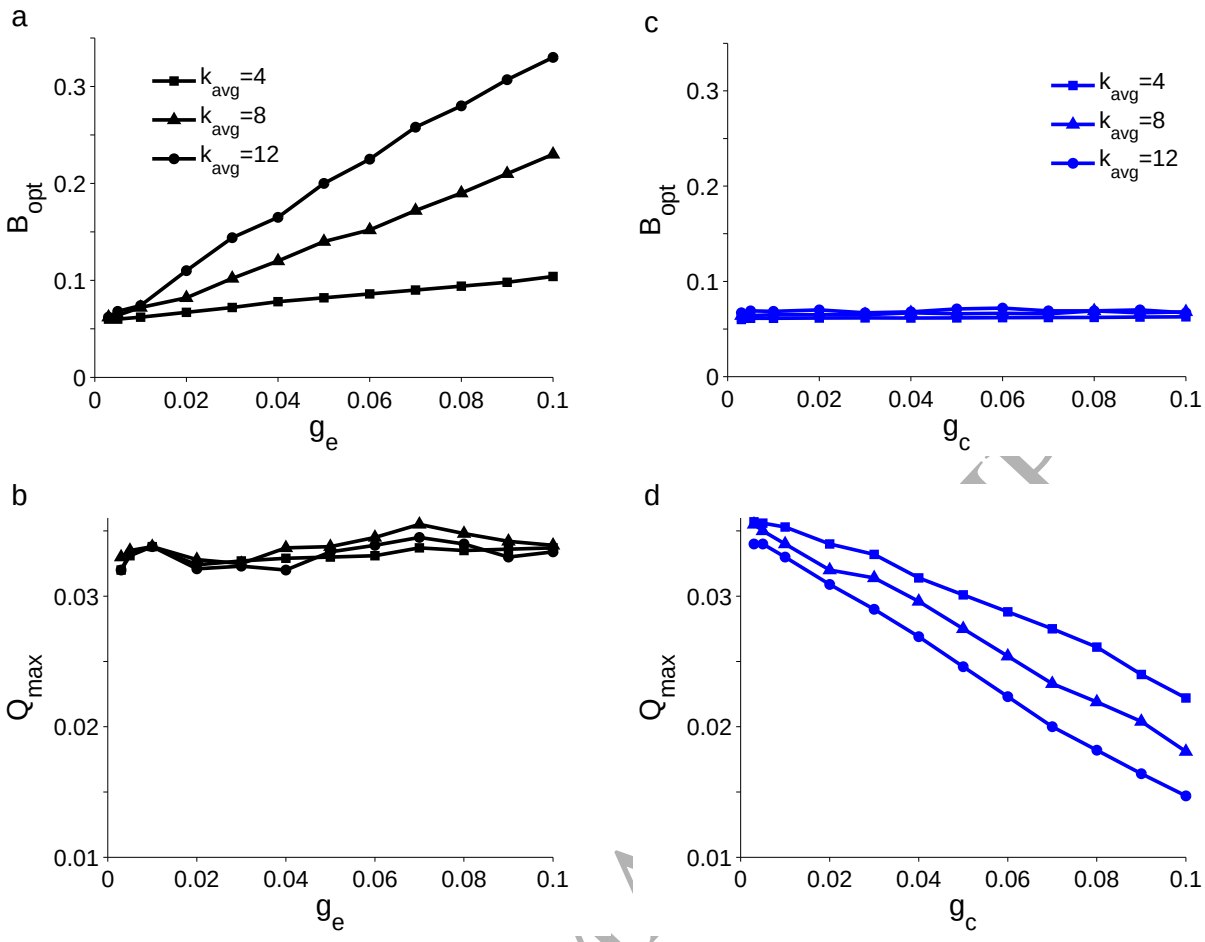


Figure 2: The influence of link density varied via the average degree $k_{\rm avg}$ and synaptic strengths ($g_{\rm e}$ and $g_{\rm c}$) on the signal detection quality ($Q_{\rm max}$) and optimal required energy level ($B_{\rm opt}$) in electrically and chemically coupled unweighted networks. Panels (a) and (b) show the variations of $B_{\rm opt}$ and $Q_{\rm max}$, respectively, as a function of $g_{\rm e}$ for different values of $k_{\rm avg}$ in electrically coupled unweighted population. Panels (c) and (d) show the similar analysis as in (a) and (b) for chemically coupled unweighted neural populations. Other model parameters as in Fig. 1.

prominent in densely coupled networks than in sparser ones (Fig. 2a). However, the quality of amplification remains almost the same with regards to changes in $g_{\rm e}$ (Fig. 2b). On the other hand, in the case of chemically coupled unweighted populations, variation of $g_{\rm c}$ does not affect the optimal energy level $B_{\rm opt}$ (Fig. 2c) regardless of $k_{\rm avg}$. However, its performance dramatically decreases the signal amplification quality (Fig. 2d). Note that latter effect becomes more prominent as the number of connections increases in chemically coupled populations.

Since the neural populations have not only complex network topologies but also weighted

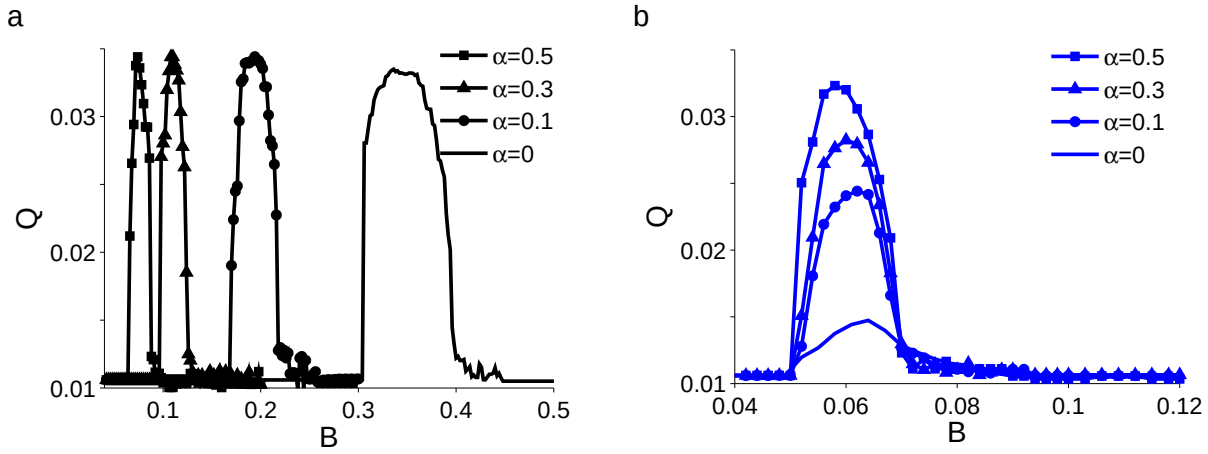


Figure 3: The influence of weighting on VR in electrically and chemically coupled neural populations. The panels demonstrate the variation of Q as a function of B for different values of weighting parameter α in (a) electrically and (b) chemically coupled populations. Parameters: $g_e = g_c = 0.1$ and $k_{avg} = 12$ in both cases. Other parameters as in Fig. 1.

communication paths, it is crucial to study the VR behavior in weighted networks in order to understand the VR dynamics in actual neural medium. This also offers insight into how weighting of connections within the population affects the weak-signal encoding efficiency of electrical and chemical synapses. For this purpose, we consider a dense and strongly coupled network configuration with $k_{avg} = 12$ and $g_e = g_c = 0.1$, and then compute the response of the networks Q as a function of B for different weighting levels by tuning the parameter α.

The obtained results are presented in Fig. 3a for electrically and in Fig. 3b for chemically coupled populations. It can be seen that weighting the connections in electrically coupled population does not significantly affect the VR performance since the maximum Q-values remain almost same for any weighting level. On the other hand, as the value of α increases, the optimal high-frequency driving amplitude B_{opt} required for the best VR performance gradually decreases for a given link density and coupling strength. This indicates that an electrically coupled neural population having weighted connections needs less energy to amplify weak-signals via the VR mechanism. Note that although there is a pronounced reduction in the required energy level, the range of B-values, for which the weak-signal is efficiently amplified, becomes smaller for larger α. This indicates a limitation of the energy range suitable for the emergence of VR in weighted electrically coupled populations. We also perform the same analysis for the case of chemically coupled neural populations. Figure 3b

ACCEPTED MANUSCRIPT

shows that weighting in chemically coupled populations affects weak-signal processing differently compared to electrically coupled neural populations. As the weighting parameter α increases, the network response Q also increases, implying a significant enhancement in VR performance of the populations. However, the optimal high-frequency driving amplitude $B_{\rm opt}$ does not change very much with variation of weighting level in the network.

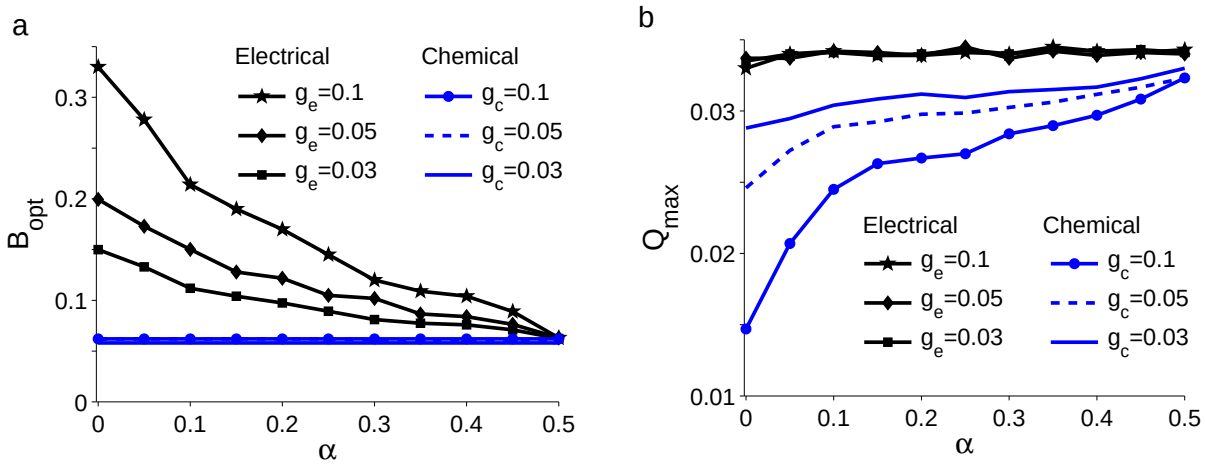


Figure 4: The influence of weighting parameter α and synaptic strength on the signal detection quality ($Q_{\rm max}$) and optimal required energy level ($B_{\rm opt}$) in electrically and chemically coupled weighted populations. Panels (a) and (b) show the variation of $B_{\rm opt}$ and $Q_{\rm max}$, respectively, as a function of α in both types of population for fixed mean degree $k_{\rm avg} = 12$ and different synaptic strengths. Other parameters as in Fig. 1.

To extend the above findings, we calculate the optimal required energy level $B_{\rm opt}$ and the maximal amplification factor $Q_{\rm max}$ as a function of the weighting parameter α for different synaptic strengths of both electrical and chemical coupled populations. Figure 4 summarizes the obtained results. In Fig. 4a, it can be observed that regardless of weighting level and synaptic strength, the most energy efficient neural response is obtained in chemically coupled populations since $B_{\rm opt}$ remains same at a minimum value for all parameter variations. On the other hand, as the network becomes more weighted in electrically coupled populations, $B_{\rm opt}$ decreases for all $g_{\rm e}$ values and finally saturates to a minimum energy level, which is also required for chemically coupled populations. In terms of signal detection quality, weighting the network in electrically coupled populations has neither a promoting nor a suppressing role at any given $g_{\rm c}$ but it significantly increases $Q_{\rm max}$ indicating an enhancement in the weak-signal encoding capability of the populations. Thus, our results suggest that the

energy dependence of VR in electrically coupled populations is not as strong as in the case of unrealistic unweighted networks. Moreover, a poor weak-signal encoding quality in a chemically coupled could be high, if the connections weights are considered in a SF network.

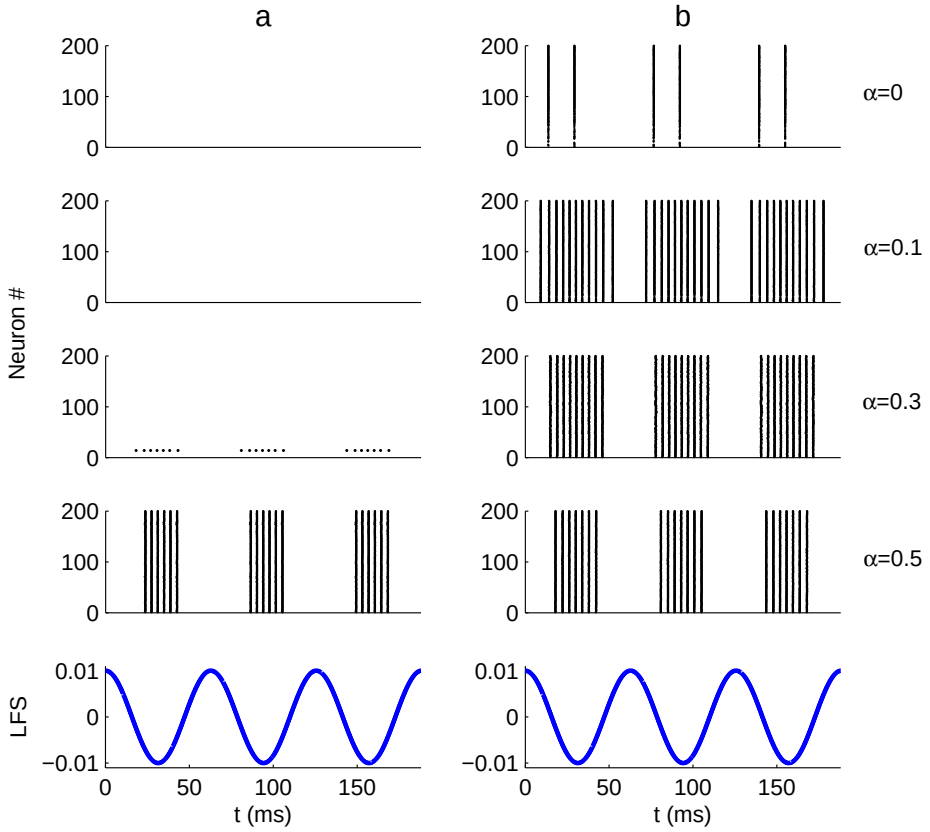


Figure 5: The influence of weighting on the response of electrically and chemically coupled populations. (a) The panels show the firing patterns of electrically coupled populations in response to a low-frequency periodic stimulation (bottom panel) as the weighting parameter α varies. (b) Similar analysis as in (a) for chemically coupled populations. Note that the presented firing patterns are obtained for a fixed high-frequency driving amplitude $B = 0.06$. Other parameters as in Fig. 3.

A qualitative understanding on different effects of weighting in electrically and chemically coupled populations can be gained by analyzing the spatio-temporal response patterns of the neurons. Figure 5 shows raster plots for different values of the weighting parameter α for a fixed HFS amplitude of $B = 0.06$, which eventually provides maximal Q for each population types (Fig. 3). In the case of electrically coupled neural populations (Fig. 5a), it can be seen that there is no spiking activity in response to input signals in unweighted networks ($\alpha = 0$). Increasing α to a certain extent cannot trigger neural activity indicating

that LFS signal is not detected by the population in the presence of HFS. However, when the weighting parameter is set to $\alpha = 0.5$, all neurons fire synchronously in correlation with the negative phase of LFS implying a successful detection and transmission of the weak input signal. We observe a different dynamical behavior in chemically coupled network where neurons fire coherently regardless of weighting level in the network. However, the correlation between LFS signal and collective spiking varies with α. More precisely, as seen in Fig. 5b, synchronized spiking columns appear during both phases of LFS resulting in lower Q-values. As the network becomes more weighted, the number of firing events in positive phase of LFS decreases. Then, all neurons start to fire only during the negative LFS phase. Such a locked mode of spiking activity into a single signal phase, either negative or positive, provides relevant information about LFS.

IV. CONCLUSIONS

We have investigated vibrational resonance in excitable FitzHugh-Nagumo systems coupled in a scale-free network via electrical gap junctions and chemical synapses. We have found that the detection performance of weak low-frequency signals is influenced by specifics of the considered coupling scheme. The underlying mechanism responsible for these different behaviors in weighted and unweighted populations may be described in terms of the optimal required energy level B_{opt} and strongest response factor Q. The unweighted network is constructed with densely and strongly coupled identical neurons with a fixed excitability parameter $a = 1.05$. From early studies of VR in single neurons [17, 18, 29, 57], it is known that the optimal HFS amplitude for a FitzHugh-Nagumo model neuron to encode a low-frequency signal via the vibrational resonance mechanism is $B_{\text{opt}} \approx 0.06$ for $a = 1.05$. In our analysis, since the considered populations have dense and strong network connections, the total synaptic current introduced into each FitzHugh-Nagumo neuron in electrically coupled networks becomes very large. This provides a permanently increased mean value of membrane potentials, which consequently increases the spiking threshold of each neurons by modulating the excitability parameter a. Therefore, neurons in unweighted electrically coupled populations stay in a quiescent state in response to low-frequency signals because each neuron needs more energy to be attracted into the basin of the spiking state. On the other hand, since the transmission via chemical synapses is controlled by a time constant

τ_{syn} of the neurotransmitter-release [58–60], the increase in the average membrane potential of neurons is not as high as in the case of electrically coupled populations. Thus, the excitability level of neurons is less effected by the total synaptic inputs. This is the reason why we have observed sparse synchronous firings in unweighted chemically coupled populations. After introducing weights into synaptic connections, the total synaptic current for each neuron is significantly reduced proportional to the node degree of each unit in the network because of scaled synaptic strengths. This means that neurons in both types of coupling start to become independent from the network. Thus, above mentioned disadvantageous of unweighted networks – high energy dependence and low signal amplification quality in electrically and chemically coupled populations, respectively – can be removed as the weighting level increases in the network.

Note that results on vibrational resonance dynamics in neural populations have been reported mostly based on networks of electrically coupled units [17, 39, 61]. A few study have also considered chemical synapses by considering trivial network configurations [18, 29, 34]. Here, we have shown the existence of vibrational resonance in chemically coupled neural populations and compared it with electrically coupled ones in scale-free networks. Although previous works stated that electrical synapses are more efficient for signal detection in neural populations than chemical ones, our results have revealed that one can achieve the same vibrational resonance performance in both coupling schemes if the features of the scale-free network are fine-tuned. Additionally, we have suggested that both coupling types in a given network have relative advantages with respect to each other by means of energy requirements and maximal signal encoding achievements. Thus, it can be concluded that network topology should be taken into account to determine the role of coupling type on the weak-signal detection capability of a neural population by vibrational resonance.

In this work, we focussed on class II excitability for the single neuronal dynamics in a given population. Since neurons with class I and III excitabilities are also ubiquitous in the brain [62, 63], a possible extension of the current work should investigate VR in electrically and chemically coupled neuronal networks by considering class I and III excitability for single neuronal dynamics. This is important, as the dynamics of populations composed of neurons with different excitability characteristics have been shown to exhibit different behaviors at the population level [64–66]. Furthermore, we considered only excitatory synapses for chemically coupled populations. It will also be interesting and insightful to further in-

vestigate whether different chemical coupling schemes (i.e., excitatory-inhibitory and purely inhibitory coupled populations) perform different roles in regulating vibrational resonance in weighted and unweighted neuronal networks.

Acknowledgments

PH acknowledges the support by *Deutsche Forschungsgemeinschaft* (DFG) in the framework of Collaborative Research Center 910.

[1] L. Gammaitoni, P. Hänggi, P. Jung, and F. Marchesoni, "Stochastic resonance," *Reviews of Modern Physics*, vol. 70, pp. 223–287, 1998.

[2] B. McNamara and K. Wiesenfeld, "Theory of stochastic resonance," *Physical Review A*, vol. 39, no. 9, p. 4854, 1989.

[3] D. F. Russell, L. A. Wilkens, and F. Moss, "Use of behavioural stochastic resonance by paddle fish for feeding," *Nature*, vol. 402, no. 6759, p. 291, 1999.

[4] J. K. Douglass, L. Wilkens, E. Pantazelou, and F. Moss, "Noise enhancement of information transfer in crayfish mechanoreceptors by stochastic resonance," *Nature*, vol. 365, no. 6444, p. 337, 1993.

[5] V. S. Anishchenko, A. B. Neiman, F. Moss, and L. Shimansky-Geier, "Stochastic resonance: noise-enhanced order," *Physics-Uspekhi*, vol. 42, no. 1, pp. 7–36, 1999.

[6] G. Schmid, I. Goychuk, and P. Hänggi, "Stochastic resonance as a collective property of ion channel assemblies," *EPL (Europhysics Letters)*, vol. 56, no. 1, p. 22, 2001.

[7] P. Hänggi, "Stochastic resonance in biology how noise can enhance detection of weak signals and help improve biological information processing," *ChemPhysChem*, vol. 3, no. 3, pp. 285–290, 2002.

[8] M. Perc, "Stochastic resonance on excitable small-world networks via a pacemaker," *Physical Review E*, vol. 76, no. 6, p. 066203, 2007.

[9] J. F. Mejias and J. J. Torres, "Emergence of resonances in neural systems: the interplay between adaptive threshold and short-term synaptic plasticity," *PLOS ONE*, vol. 6, no. 3, p. e17255, 2011.

ACCEPTED MANUSCRIPT

[10] J. J. Torres, J. Marro, and J. F. Mejias, "Can intrinsic noise induce various resonant peaks?," *New Journal of Physics*, vol. 13, no. 5, p. 053014, 2011.

[11] G. Pinamonti, J. Marro, and J. J. Torres, "Stochastic resonance crossovers in complex networks," *PLOS ONE*, vol. 7, no. 12, p. e51170, 2012.

[12] J. J. Torres, I. Elices, and J. Marro, "Stochastic multiresonances in complex nets of spiking neurons," *International Journal of Complex Systems in Science*, vol. 3, no. 1, pp. 21–25, 2013.

[13] P. S. Landa and P. V. E. McClintock, "Vibrational resonance," *Journal of Physics A: Mathematical and General*, vol. 33, no. 45, p. L433, 2000.

[14] S. M. Meerkov, "Principle of vibrational control: Theory and applications," *IEEE Transactions on Automatic Control*, vol. 25, no. 4, pp. 755–762, 1980.

[15] S. M. Meerkov, "Vibrational control theory," *Journal of the Franklin Institute*, vol. 303, no. 2, pp. 117–128, 1977.

[16] J. M. Berg and I. P. Manjula Wickramasinghe, "Vibrational control without averaging," *Automatica*, vol. 58, pp. 72–81, 2015.

[17] B. Deng, J. Wang, X. Wei, K. M. Tsang, and W. L. Chan, "Vibrational resonance in neuron populations," *Chaos*, vol. 20, no. 1, p. 013113, 2010.

[18] J. Sun, B. Deng, C. Liu, H. Yu, J. Wang, X. Wei, and J. Zhao, "Vibrational resonance in neuron populations with hybrid synapses," *Applied Mathematical Modelling*, vol. 37, no. 9, pp. 6311–6324, 2013.

[19] G. M. Shepherd, *The Synaptic Organization of the Brain.* Oxford University Press, USA, 2004.

[20] J. D. Victor and M. M. Conte, "Two-frequency analysis of interactions elicited by vernier stimuli," *Visual Neuroscience*, vol. 17, no. 6, pp. 959–973, 2000.

[21] O. Schläfer, T. Onyeche, H. Bormann, C. Schröder, and M. Sievers, "Ultrasound stimulation of micro-organisms for enhanced biodegradation," *Ultrasonics*, vol. 40, no. 1-8, pp. 25–29, 2002.

[22] M. Perc and M. Marhl, "Amplification of information transfer in excitable systems that reside in a steady state near a bifurcation point to complex oscillatory behavior," *Physical Review E*, vol. 71, no. 2, p. 026229, 2005.

[23] J. W. Middleton, A. Longtin, J. Benda, and L. Maler, "The cellular basis for parallel neural transmission of a high-frequency stimulus and its low-frequency envelope," *Proceedings of the*

ACCEPTED MANUSCRIPT

National Academy of Sciences USA, vol. 103, no. 39, pp. 14596–14601, 2006.

[24] W. Heiligenberg, *Neural nets in electric fish*. MIT press Cambridge, MA, 1991.

[25] T. Pereira, M. S. Baptista, and J. Kurths, "Multi-time-scale synchronization and information processing in bursting neuron networks," *The European Physical Journal Special Topics*, vol. 146, no. 1, pp. 155–168, 2007.

[26] X.-X. Wu, C. Yao, and J. Shuai, "Enhanced multiple vibrational resonances by Na^+ and K^+ dynamics in a neuron model," *Scientific Reports*, vol. 5, p. 7684, 2015.

[27] T. O. Roy-Layinde, J. A. Laoye, O. O. Popoola, and U. E. Vincent, "Analysis of vibrational resonance in bi-harmonically driven plasma," *Chaos*, vol. 26, no. 9, p. 093117, 2016.

[28] E. Ullner, A. Zaikin, J. Garcıa-Ojalvo, R. Bascones, and J. Kurths, "Vibrational resonance and vibrational propagation in excitable systems," *Physics Letters A*, vol. 312, no. 5, pp. 348–354, 2003.

[29] B. Deng, J. Wang, and X. Wei, "Effect of chemical synapse on vibrational resonance in coupled neurons," *Chaos*, vol. 19, no. 1, p. 013117, 2009.

[30] Y.-M. Qin, J. Wang, C. Men, B. Deng, and X.-L. Wei, "Vibrational resonance in feedforward network," *Chaos*, vol. 21, no. 2, p. 023133, 2011.

[31] M. Xue, J. Wang, B. Deng, and X. Wei, "Vibrational resonance in feedforward neuronal network with unreliable synapses," *The European Physical Journal B*, vol. 86, no. 4, pp. 1–9, 2013.

[32] Y. Qin, C. Han, Y. Che, and J. Zhao, "Vibrational resonance in a randomly connected neural network," *Cognitive Neurodynamics*, pp. 1–10, 2018.

[33] H. Yu, X. Guo, J. Wang, B. Deng, and X. Wei, "Vibrational resonance in adaptive small-world neuronal networks with spike-timing-dependent plasticity," *Physica A*, vol. 436, pp. 170–179, 2015.

[34] H. Yu, J. Wang, J. Sun, and H. Yu, "Effects of hybrid synapses on the vibrational resonance in small-world neuronal networks," *Chaos*, vol. 22, no. 3, p. 033105, 2012.

[35] P. Ciuciu, P. Abry, and B. J. He, "Interplay between functional connectivity and scale-free dynamics in intrinsic fMRI networks," *NeuroImage*, vol. 95, pp. 248–263, 2014.

[36] J.-P. Thivierge, "Scale-free and economical features of functional connectivity in neuronal networks," *Physical Review E*, vol. 90, no. 2, p. 022721, 2014.

[37] X. Li, G. Ouyang, A. Usami, Y. Ikegaya, and A. Sik, "Scale-free topology of the ca3 hip-

ACCEPTED MANUSCRIPT

pocampal network: a novel method to analyze functional neuronal assemblies," *Biophysical Journal*, vol. 98, no. 9, pp. 1733–1741, 2010.

[38] V. M. Eguiluz, D. R. Chialvo, G. A. Cecchi, M. Baliki, and A. V. Apkarian, "Scale-free brain functional networks," *Physical Review Letters*, vol. 94, no. 1, p. 018102, 2005.

[39] M. Uzuntarla, E. Yilmaz, A. Wagemakers, and M. Ozer, "Vibrational resonance in a heterogeneous scale free network of neurons," *Communications in Nonlinear Science and Numerical Simulation*, vol. 22, no. 1, pp. 367–374, 2015.

[40] X. Li, J. Wang, and W. Hu, "Effects of chemical synapses on the enhancement of signal propagation in coupled neurons near the canard regime," *Physical Review E*, vol. 76, no. 4, p. 041902, 2007.

[41] D. Guo and C. Li, "Stochastic and coherence resonance in feed-forward-loop neuronal network motifs," *Physical Review E*, vol. 79, no. 5, p. 051921, 2009.

[42] E. Yilmaz, M. Uzuntarla, M. Ozer, and M. Perc, "Stochastic resonance in hybrid scale-free neuronal networks," *Physica A: Statistical Mechanics and its Applications*, vol. 392, no. 22, pp. 5735–5741, 2013.

[43] J. Wang, X. Guo, H. Yu, C. Liu, B. Deng, X. Wei, and Y. Chen, "Stochastic resonance in small-world neuronal networks with hybrid electrical–chemical synapses," *Chaos, Solitons & Fractals*, vol. 60, pp. 40–48, 2014.

[44] D. Guo, M. Perc, Y. Zhang, P. Xu, and D. Yao, "Frequency-difference-dependent stochastic resonance in neural systems," *Physical Review E*, vol. 96, no. 2, p. 022415, 2017.

[45] L. E. Roberts, J. J. Eggermont, D. M. Caspary, S. E. Shore, J. R. Melcher, and J. A. Kaltenbach, "Ringing ears: the neuroscience of tinnitus," *Journal of Neuroscience*, vol. 30, no. 45, pp. 14972–14979, 2010.

[46] O. Sporns, "Structure and function of complex brain networks," *Dialogues in Clinical Neuroscience*, vol. 15, no. 3, p. 247, 2013.

[47] J. Zhao, L. Miao, J. Yang, H. Fang, Q.-M. Zhang, M. Nie, P. Holme, and T. Zhou, "Prediction of links and weights in networks by reliable routes," *Scientific Reports*, vol. 5, p. 12261, 2015.

[48] G. Mei, X. Wu, G. Chen, and J.-A. Lu, "Identifying structures of continuously-varying weighted networks," *Scientific Reports*, vol. 6, p. 26649, 2016.

[49] D. Batalle *et al.*, "Early development of structural networks and the impact of prematurity on brain connectivity," *NeuroImage*, vol. 149, pp. 379–392, 2017.

ACCEPTED MANUSCRIPT

[50] R. FitzHugh, "Impulses and physiological states in theoretical models of nerve membrane," *Biophysical Journal*, vol. 1, no. 6, pp. 445 – 466, 1961.

[51] M. Uzuntarla, E. Barreto, and J. J. Torres, "Inverse stochastic resonance in networks of spiking neurons," *PLOS Computational Biology*, vol. 13, no. 7, p. e1005646, 2017.

[52] J. Wang, X. Zuo, and Y. He, "Graph-based network analysis of resting-state functional MRI," *Frontiers in Systems Neuroscience*, vol. 4, p. 16, 2010.

[53] P. J. Macdonald, E. Almaas, and A.-L. Barabási, "Minimum spanning trees of weighted scale-free networks," *EPL (Europhysics Letters)*, vol. 72, no. 2, p. 308, 2005.

[54] A. Barrat, M. Barthélemy, R. Pastor-Satorras, and A. Vespignani, "The architecture of complex weighted networks," *Proceedings of the National Academy of Sciences USA*, vol. 101, no. 11, pp. 3747–3752, 2004.

[55] A.-L. Barabasi and R. Albert, "Emergence of scaling in random networks," *Science*, vol. 286, no. 5439, pp. 509–512, 1999.

[56] W.-X. Wang, L. Huang, Y.-C. Lai, and G. Chen, "Onset of synchronization in weighted scale-free networks," *Chaos*, vol. 19, no. 1, p. 013134, 2009.

[57] B. Deng, J. Wang, X. Wei, H. Yu, and H. Li, "Theoretical analysis of vibrational resonance in a neuron model near a bifurcation point," *Physical Review E*, vol. 89, no. 6, p. 062916, 2014.

[58] S. P. Gandhi and C. F. Stevens, "Three modes of synaptic vesicular recycling revealed by single-vesicle imaging," *Nature*, vol. 423, no. 6940, p. 607, 2003.

[59] D. Guo, Q. Wang, and M. Perc, "Complex synchronous behavior in interneuronal networks with delayed inhibitory and fast electrical synapses," *Physical Review E*, vol. 85, no. 6, p. 061905, 2012.

[60] A. J. Arnold, A. Razavieh, J. R. Nasr, D. S. Schulman, C. M. Eichfeld, and S. Das, "Mimicking neurotransmitter release in chemical synapses via hysteresis engineering in mos2 transistors," *ACS Nano*, vol. 11, no. 3, pp. 3110–3118, 2017.

[61] H. Yu, J. Wang, C. Liu, B. Deng, and X. Wei, "Vibrational resonance in excitable neuronal systems," *Chaos*, vol. 21, no. 4, p. 043101, 2011.

[62] S. A. Prescott, Y. De Koninck, and T. J. Sejnowski, "Biophysical basis for three distinct dynamical mechanisms of action potential initiation," *PLOS Computational Biology*, vol. 4, no. 10, p. e1000198, 2008.

[63] D. Guo, S. Wu, M. Chen, M. Perc, Y. Zhang, J. Ma, Y. Cui, P. Xu, Y. Xia, and D. Yao,

ACCEPTED MANUSCRIPT

"Regulation of irregular neuronal firing by autaptic transmission," *Scientific Reports*, vol. 6, p. 26096, 2016.

[64] E. M. Izhikevich, "Neural excitability, spiking and bursting," *International Journal of Bifurcation and Chaos*, vol. 10, no. 06, pp. 1171–1266, 2000.

[65] C. G. Fink, V. Booth, and M. Zochowski, "Cellularly-driven differences in network synchronization propensity are differentially modulated by firing frequency," *PLOS Computational Biology*, vol. 7, no. 5, p. e1002062, 2011.

[66] D. Guo, M. Chen, M. Perc, S. Wu, C. Xia, Y. Zhang, P. Xu, Y. Xia, and D. Yao, "Firing regulation of fast-spiking interneurons by autaptic inhibition," *EPL (Europhysics Letters)*, vol. 114, no. 3, p. 30001, 2016.

ACCEPTED MANUSCRIPT

ACCEPTED MANUSCRIPT

Biography



Sukruye Nihal Agaoglu received her B.Sc. degree in Electronics and Communication Engineering from Kocaeli University, Kocaeli, Turkey, in 2004, the M.S. degree in Electrical and Electronics Engineering from Bulent Ecevit University, Zonguldak, Turkey, in 2006. She is currently pursuing the Ph.D. degree in Electrical and Electronics Engineering at Bulent Ecevit University, Zonguldak, Turkey. Her research interest is primarily in computational neuroscience and medical electronics.



Ali Calim received his B.Sc. degree in Electrical and Electronics Engineering from Bahcesehir University, Istanbul, Turkey, in 2009, the M.S. degree in Electrical and Electronics Engineering from Bulent Ecevit University, Zonguldak, Turkey, in 2014. He is currently a Research Assistant in the Department of Biomedical Engineering at Bulent Ecevit University and, pursuing the Ph.D. degree Electrical and Electronics Engineering at Bulent Ecevit University, Zonguldak, Turkey. His research interests include topics in computational neuroscience and medical electronics.



Philipp Hövel received his academic degrees from Technische Universität Berlin, Germany: Diplomas in Physics (2004) and Mathematics (2006), PhD in physics (2009), Habilitation in Theoretical Physics (2017). He is currently a permanent lecturer in the School of Mathematical Sciences at University College Cork, Ireland. His research mission is to lift the boundaries between data-oriented science, theoretical approaches, and numerical simu-

lations addressing interdisciplinary questions in the overlap of nonlinear dynamics, network science, and control theory.



Mahmut Ozer received his B.Sc. degree in Electronics and Communication Engineering from Istanbul Technical University, Istanbul, Turkey, in 1992 and, the Ph.D. degree in Electronics Engineering from Karadeniz Technical University, Trabzon, Turkey, in 2001. He is currently a Professor of Electrical and Electronics Engineering at Bulent Ecevit University in Zonguldak, Turkey. His research interests include biomedical, electronic circuits, biophysics and computational neuroscience.



Muhammet Uzuntarla received his B.Sc. degree in Electronics and Communication Engineering from Kocaeli University, Kocaeli, Turkey, in 2003, the M.S. degree in Electrical and Electronics Engineering from Bulent Ecevit University, Zonguldak, Turkey, in 2006 and the Ph.D. degree in Electrical and Electronics Engineering from Sakarya University, Sakarya, Turkey, in 2011. He is currently an Associate Professor of Biomedical Engineering at Bulent Ecevit University in Zonguldak, Turkey. His research interests include nonlinear systems, computational neuroscience and medical electronics.

ACCEPTED MANUSCRIPT